A full scale experimental investigation of passenger and freight train aerodynamics

Soper, David; Baker, Christopher

DOI:
10.1177/0954409719844431

Document Version
Peer reviewed version

Citation for published version (Harvard):
Soper, D & Baker, C 2019, 'A full scale experimental investigation of passenger and freight train aerodynamics', *Proceedings of the Institution of Mechanical Engineers, Part F: Journal of Rail and Rapid Transit*. https://doi.org/10.1177/0954409719844431

A full scale experimental investigation of passenger and freight train aerodynamics

David Soper, Chris Baker

Abstract

The movement of a train creates a disturbance to air through which it passes, known as a slipstream. Such disturbances are characterised by changes in pressure, notably around the vehicle nose/tail, and highly turbulent boundary growth along the vehicle side with increasing slipstream velocity magnitude. Although these characteristic features occur in some form for all trains, the flow development associated with various train types can often be very different. Variability in train type makes it difficult to accurately characterise aerodynamic effects of each individual train. In this paper a detailed set of tests are undertaken to assess the aerodynamic flow development created around various train types common to the UK railway network. Comparison of analysed data from different passenger and freight trains was made. The variability of freight train results was larger in comparison to passenger trains examined, caused by large flow separations around the bluff freight train. Although train speeds were lower for the freight train, slipstream velocity and pressure magnitudes were larger than observed for passenger trains. Passenger trains could be divided aerodynamically into two main types; long distance passenger trains and commuter trains. Longer train lengths were shown to increase the boundary layer growth; an important feature for long distance passenger trains as it creates an increase in the slipstream velocity peak magnitude at the train tail. Boundary layer stabilisation is not observed as in previous studies. The coupling of two carriage sets together, creating a large V-shaped region at the centre of the train, led to a clear step slipstream velocity peak coinciding with the change in pressure at the coupling region. Cross-correlation of results from measuring positions within the characteristic turbulent length scale range appeared to show similar results to autocorrelation time scales for larger scale separation of turbulent structures from bogie and inter-carriage regions.

1 Introduction

The movement of a train creates a disturbance to air through which it passes, known as a slipstream [3]. Such disturbances are characterised by changes in pressure, notably around the vehicle nose/tail, and a highly turbulent boundary growth along

Nomenclature

$\overline{U_{2\sigma}}$	Non-dimensional TSI value	T	normalised time nominal height 4 m
$\overline{u_{2\sigma}}$	Dimensional TSI value (m/s)	t	Time (s)
$\overline{u_{max}}$	Maximum 1 second moving average value	U	Normalised longitudinal velocity
ρ	air density (kg/m^3)	u	ensemble mean of longitudinal slipstream velocity (m/s)
σ	Standard deviation of peak velocities (m/s)	U_{res}	overall normalised horizontal velocity
τ	Normalised time scale by carriage length	V	Normalised lateral velocity
C_P	coefficient of pressure	v	ensemble mean of lateral slipstream velocity (m/s)
I	turbulence intensity	V_{train}	train speed (m/s)
L_{train}	train length (m)	x_{nl}	nose length (m)
p	measured pressure (Pa)		
p_0	ambient pressure (Pa)		

the vehicle side with increasing slipstream velocities. It is known that these aerodynamic effects increase, approximately, with a squared relationship; as such consequently at higher speeds aerodynamic effects will be significantly greater than for vehicles travelling at lower speeds [4]. This statement is true for increasing vehicle speeds when the vehicle itself is kept constant but can become 'blurred' when comparing different vehicle types. It is however important to understand the developing aerodynamic flow around railway vehicles to ensure safety for passengers and trackside workers, as well as fatigue loads on trackside structures.

The UK rail network has a wide variety of traffic ranging from high-speed passenger and slower commuter trains, to freight and maintenance trains, as well as heritage activities. Indeed, in many cases this traffic utilises different types of rail vehicles in various configurations with differing train lengths, travelling at different train speeds. Such variability makes it difficult to accurately characterise the aerodynamic effects of each individual train type at any one moment in time. The need for interoperability for rail operators across Europe has led to the development of a series of Technical Specifications for Interoperability (TSI) for rolling stock in different countries, which include safe operational limits on train aerodynamics [35].

Full scale studies are by nature complex, expensive and time consuming to undertake; however, such studies are vital for understanding highly turbulent flows. Railway aerodynamics in the UK is built upon model scale experiments [3, 29, 7] and numerical simulations [13, 19, 12] but full scale work is vitally important for validation of different modelling techniques. Previous full scale studies [20, 33, 34, 5] have been conducted by railway authorities either in response to an aerodynamic incident or to aid production of standards in relation to operation and safety [35]. These studies have tended to focus on a small number of specific train types, generally considered as generic trains within categories of train speed, without comparing the variation of traffic observed on the rail networks. More recently knowledge of railway aerodynamics has dramatically increased due to work conducted by universities and private research groups, both experimentally and numerically across a wide range of scales and topics [25]. All this work has fed into a number of large scale European projects, namely the RAPIDE (Railway Aerodynamics of Passing and Interaction with Dynamic Effects), AOA (Aerodynamics in the Open Air) and AeroTRAIN projects [26, 32, 10, 4]. Many of the results from these studies have fed into national and international standards [9, 8] and the TSI [35].

Certification for new rolling stock that will travel at speeds faster than 160 km/h must follow a series of standards on vehicle aerodynamics in the open air set out in the TSI and CEN standards [9, 35], conducted through either full scale or model scale testing, and or numerical simulations. Rocchi et al. [25] have directly applied this approach in the certification of a new High Speed Italian train, focusing on key aerodynamic properties, such as head pressure pulses, loads on noise barriers, slipstream effects beside the track and aerodynamic loads on the trackbed. This methodology has been proven to be suitable for assessing new train designs and further optimisation of train designs in relation to the key aerodynamic properties discussed. However, due to the nature of traffic on the UK rail network

and the variability created within highly complex turbulent aerodynamic flows, the aerodynamics of railway vehicles is still not widely understood within the greater railway industry.

This paper presents data collected by staff at University of Birmingham (UoB) during a series of aerodynamic tests conducted on the West Coast Main Line (WCML), UK, to assess how freight trains fit within current TSI standards on railway operation. Consequently, the 3 day test recorded aerodynamic data for every train that passed the measuring site, creating a large data set with a cross section of typical UK train types. In this paper a detailed analysis of passenger train data will be conducted with comparisons drawn with the freight data. An additional paper will also be published in the future to further investigate findings in relation to freight trains. The test site and experiment methodology is presented in section 2. The techniques and methodology for analysing the data are discussed in section 3. An overview of the aerodynamic flow created by the various common train types recorded is given in section 4.1. Section 4 presents a comparison and analysis of the effects of train length, nose pressure and slipstream velocity peaks and the turbulent structures in the boundary layer region.

2 Experiment methodology

2.1 Test site

Acton Bridge Network Rail (NR) maintenance yard is situated next to the UP (in the direction of London) track of the West Coast Main Line (WCML), close to the small station located in the Cheshire village of Acton Bridge, UK. There are three tracks through the station; two fast lines (max speed 200 km/h for passenger trains and 120 km/h for freight) and a slow line (max speed 65 km/h rising to 80 km/h following the southern end of the platform). To the north of the maintenance yard,

before the crossover at the beginning of the slow line, is a flat area of land used for the experiment (shown in figures 1 and 2). Acton Bridge station was previously used by British Rail to conduct experiments on slipstream magnitudes of freight trains carrying transit vans to help design safety precautions [24].

Figure 1: An aerial view of Acton Bridge and the experiment site.

The site has a 300-400 mm high ballast shoulder falling to a flat section of ballast, bounded by a small footpath, figure 2. The flat area was ideal for positioning the measuring equipment stands. The test site also contained a permanent welfare cabin from which the experiments could be monitored and changes in ambient conditions recorded.

(a) Facing north (b) Facing south

Figure 2: The experiment site.

2.2 Train types

A large variety of rail traffic was observed passing the experiment test site. This paper will mainly focus on the different types of passenger trains recorded, as well as the Royal Mail postal Class 325 freight train and a collation of freight data hauled by a Class 66 locomotive. The non-standardised nature of freight traffic makes analysis difficult in relation to passenger trains. Table 1 gives an overview of the characteristic details of each train analysed.

	Train type					
	Class 66	Class 90 sleepers	Class 221	Class 325	Class 350	Class 390
						
Train speed (kph)	120	120	200	160	160	200
Approx train length (m)	550	378	121.3 or 242.6	240	80	217.5 or 265.3
Number of carriages	-	12 or 16	5 or 10	12	4	9 or 11
Number of runs	24	6	9	8	48	60

Table 1: Types of passenger and freight trains analysed.

2.3 Aerodynamic instrumentation

The aim of this experiment was to collect a large set of aerodynamic slipstream velocity data recorded at the measuring positions laid out in the TSI [35]. A series of pressure probes, used as a method to align data with respect to test site bounds, also enabled slipstream static pressures to be recorded. Recorded data was processed within a set of bounds on ambient conditions [9], monitored by atmospheric condition instrumentation. All instrumentation is discussed in detail below in relation to the aerodynamic or atmospheric property measured.

2.3.1 Slipstream velocities

Gill Instruments type R3-50 and R3-100 ultrasonic anemometers (USAs) were positioned in the cess (the area to the side of a railway track) to measure slipstream velocities. The anemometers are capable of measuring 3-components of velocity and the mean flow direction at a sampling frequency of 50 or 100 Hz, depending on the model type. The USAs were connected to small AntiLog RS232 data loggers and powered using 12 Volt deep cycle batteries. An arrangement of scaffolding poles were used to mount the probes horizontally towards the track, ensuring that the potential collapse radius did not encroach on the nearest rail. The positions tested are all prescribed measurement positions in the TSI Regulation 1302/2014 document [35], and are summarised in table 3.

A single USA setup is shown in figure 3(a). The measuring positions were repeated at 4 m intervals to allow multiple measurements to be made for each train pass. CEN standards [9] state measuring instrumentation should be repeated at a minimum of 20 m intervals to negate any possible interactions between instrumentation and ensure measurements are independent. This was however not possible in this test due to confines of the test site and the overhead line stanchions. Given the number of train passes for each train type, shown in table 1, it was necessary

to use data from all probes to ensure the ensemble size was as large as possible. It should be noted that for train types where insufficient runs for CEN purposes are recorded, there is an increased uncertainty associated with the analysis of these measurements, as discussed throughout the results sections. For the data presented, it is expected that interactions between instrumentation would be negligible due to the size of the probe head.

(a) USAs (b) Static pressure probes (c) Reference USA

Figure 3: Measuring instrument setup. (a) The ultrasonic anemometer setup at measuring heights 0.2 m and 1.4 m above the top of rail. (b) The static pressure probe setup at measuring heights 0.9 m and 1.2 m above the top of rail. (c) Reference wind speed ultrasonic anemometer setup 12.65 m from the centre of track at 3 m above the ground level.

2.3.2 Static pressures of the slipstream

At positions either side of the trackside USA's, static pressure probes were setup to act as a method of aligning data, calculating train speed and to measure the static pressure transients due to the passing trains. The probes were designed by Hoxey et al [16] as a method of easily measuring the static pressure on the surface of a building without the need of creating a pressure tap. These probes have been shown to record static pressure of slipstreams around a train accurately in previous studies [21, 27]. The probes were mounted at two measuring heights, as shown in table 3

and figure 3(b), directly to a scaffolding pole. These probe positions were repeated at each end of the site and separated by 16.2 m. It should be noted that it was not possible to place the probes at the positions defined in the CEN standards due to restrictions on the collapse radius of the probe mounts to the nearest rail.

The static pressure probes were connected, via pneumatic tubing, to custom built data logger units positioned in protective instrumentation boxes in the cess. The data loggers are designed to record pressure signals digitally at a sampling frequency of 256 Hz, saving data directly to an in built SSD card. The instrumentation was also powered by deep cycle 12 Volt rechargeable batteries that were periodically rotated throughout the test. First Sensor SQ276-43EB pressure transducers were mounted directly to the logger PCB board and pneumatic tubes used to connect the measuring ports of the transducers to adapters built into the side of the data logger casing. All transducer reference pressure ports were connected to a common manifold which was connected to a long pneumatic tube fed away from the track to area on the far side of the test site, away from any influence of passing trains. A static pressure probe was mounted to the end of the reference pressure tubing to protect the tube from rainfall and insects.

2.3.3 Reference wind speed

A Gill Instruments 10 Hz USA provided ambient reference wind speed measurements at a position 12.65 m from centre of track at a height of 3 m above the ground level, shown in figure 3(c). This position was chosen as a suitable location away from the influence of the train slipstreams. The USA was connected to a small AntiLog RS232 data logger and powered using 12 Volt deep cycle batteries. Atmospheric reference values for air temperature, humidity and pressure were measured using a GBP3300 Digital Barometer and an Oregon Scientific BAR208HGA. Values were recorded periodically throughout the test in relation to changes in at-

mospheric conditions.

2.3.4 Identification of train type, speed and location

A video camera was set up throughout the test period to record each train passage, enabling the train type and consist to be identified in the processing phase. A radar speed gun was used to determine the train speed, providing a method of comparison to the static pressure speed calculation.

2.3.5 Summary of measuring instrumentation locations

Table 3 summarises the sensor positions for the trackside test.

Measurement type	Lateral measurement distance from centre of track (m)	Measurement height above top of rail (m)	Distance from 1st pressure probe (m)	Instrument type
Slipstream velocity	3 m	0.2 m	3.90 m	50 Hz USA
	3 m	0.2 m	8.05 m	50 Hz USA
	3 m	0.2 m	12.72 m	50 Hz USA
	3 m	1.4 m	3.90 m	50 Hz USA
	3 m	1.4 m	8.05 m	100 Hz USA
	3 m	1.4 m	12.72 m	100 Hz USA
Static pressure	3 m	0.9 m	0 m	Static pressure probe
	3 m	1.2 m	0 m	Static pressure probe
	3 m	0.9 m	16.24 m	Static pressure probe
	3 m	1.2 m	16.24 m	Static pressure probe
Reference wind	12.65 m	3.0 m above ground level	3.90 m	10 Hz USA

Table 3: Summary of instrument type and locations.

3 Analysis methodology

Data was collected for all instrumentation continuously over a 3 day period, creating a series of large data sets; an example is shown in figure 4. Initially the large data set was split into a series of files for each individual train pass by cross referencing synchronised time steps in the aerodynamic data against the Real Time Trains (RTT) database [1]. The RTT database uses measurements from a series of timing points around the UK railway network to provide an accurate record of the time of passage, vehicle type and direction of travel. The RTT data was used to split the large data sets into a series of 120 second long files centred about each train passage.

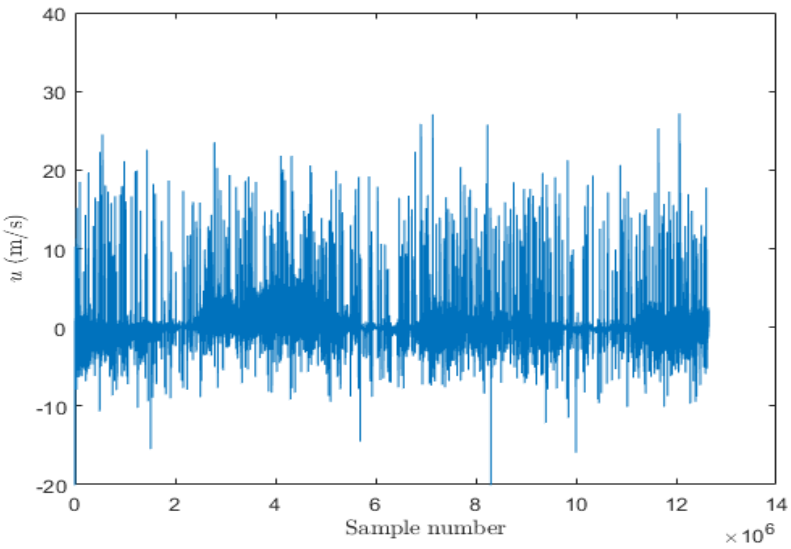

Figure 4: An example data set from an ultrasonic anemometer for the full 3 day test period. Each large peak relates to an individual train passage.

Once split into individual train passages and train type, the data was processed with respect to two cut-off values. CEN standards suggest that aerodynamic measurements should be made in ambient wind conditions below 2 m/s and that train speeds should lie within $\pm 5\%$ of the maximum permitted train speed for an indi-

vidual vehicle type [9]. By adopting these limits it was found that nearly all train passes occurred in ambient wind conditions below 2 m/s; however, train speeds were shown to fluctuate greatly. When possible CEN standards were adhered to; however, it was shown that by normalising data with respect to individual train speeds and resampling with respect to the maximum train speed for a particular train type gave results within the bounds of experimental uncertainty, in comparison to data processed directly using the methodology laid out in the CEN standards [9].

Run-to-run variations in train speed can pose issues when analysing data. As such, raw data must be resampled with respect to a nominal train speed, chosen to be the maximum line speed for each train type (table 1), to account for these differences. This method has obvious drawbacks when analysing data from long trains, where it is possible to observe variations in train speed through the test site along the train length. Analysis of static pressure peaks along the train indicated that for the majority of trains recorded that the train speeds measured were relatively constant; however those which did change beyond $\pm 10\%$ were removed from the analysis. In the following analysis, all results presented will be normalised with respect to train speed to allow the reader to compare different train types easily. The following equations show the method of normalisation,

$$U(t) = \frac{u(t)}{V_{train}} \tag{1}$$

$$V(t) = \frac{v(t)}{V_{train}} \tag{2}$$

$$U_{res}(t) = \sqrt{\left(\frac{u(t)}{V_{train}}\right)^2 + \left(\frac{v(t)}{V_{train}}\right)^2} \tag{3}$$

$$C_P(t) = \frac{p(t) - p_0}{\frac{1}{2}\rho V_{train}^2} \tag{4}$$

where t is time. U_{res} is the overall normalised horizontal velocity calculated from

longitudinal and lateral velocity components u and v. The coefficient of pressure C_P is calculated with respect to an ambient reference pressure p_0, and the air density ρ. The variation in air density about the standard value 1.225 kg/m^3, monitored by the ambient weather condition instruments, was shown to be minimal and as such the standard value was adopted.

All data was aligned so that the origin occurs when the train nose passes the measuring instrumentation, by initially aligning with respect to the positive pressure peak at the first static pressure probe and correcting with respect to the train speed and distance between each instrument position.

Previous studies have discussed the merits of applying ensemble averaging techniques as a method to analyse highly turbulent data [5]. CEN standards [9] state that 20 independent runs should be measured to form an ensemble average. However, it is sometimes not possible to obtain 20 'good' runs of data for each train type; as such the maximum number of runs recorded will be used, as shown in table 1. Ensemble averaging, by nature, effectively smooths data through removing the stochastic turbulence of individual runs. It is therefore important to also conduct detailed analysis of data from individual train passes to understand the level of fluctuations about the ensemble.

4 Results

4.1 General flow development

To thoroughly understand the detailed analysis presented in the following sections it is first important to understand the general flow development for the different train types analysed and to establish reasons for any differences observed. The general flow development around high speed passenger and freight trains has been discussed in detail in previous studies [37, 4, 6, 29, 25] and as such this analysis will

focus on the differences between the types of trains analysed. In figures 5 and 6 the calculated ensemble average time series results of slipstream velocities and static pressure are presented for each major train type analysed (long distance passenger trains - Classes 221 and 390, sleeper train - Class 90, commuter train - Class 350 and freight trains - Classes 66 and 325). The results presented are all recorded at 50 Hz (resampled when necessary for the 100 Hz probes) to give the greatest number of runs for each train type in the averaging process. Normalising the results allows a relative comparison of slipstream magnitudes, even though the different train types were travelling at different train speeds. What is initially striking is the variability of freight results in comparison to the passenger trains. Soper et al. [29] cited the major cause for this variability was separation of aerodynamic flow structures around the bluff freight train shape leading to a complex highly turbulent slipstream around the train. It should be noted that the relatively high velocities measured for the Class 325 are thought to be related to the lower ensemble size in relation to other train types; ideally more train passes would be required to create a more stable ensemble average and as such the results presented here are for illustrative purposes only for the general flow development.

The introduction of aerodynamic smoothing features to passenger trains, in line with increases in train speeds, promotes less flow separation and variability, with aerodynamic flows developing into boundary layers that remain close to the train side. It is clear that although the train speed is lower for the freight train the magnitude of the flow is larger than observed for the passenger trains. For example, peak ensemble slipstream velocity values for the Class 390 passenger train are in the region of 8 m/s, whereas for Class 66 freight train peak ensemble slipstream velocities are around 10.5 m/s.

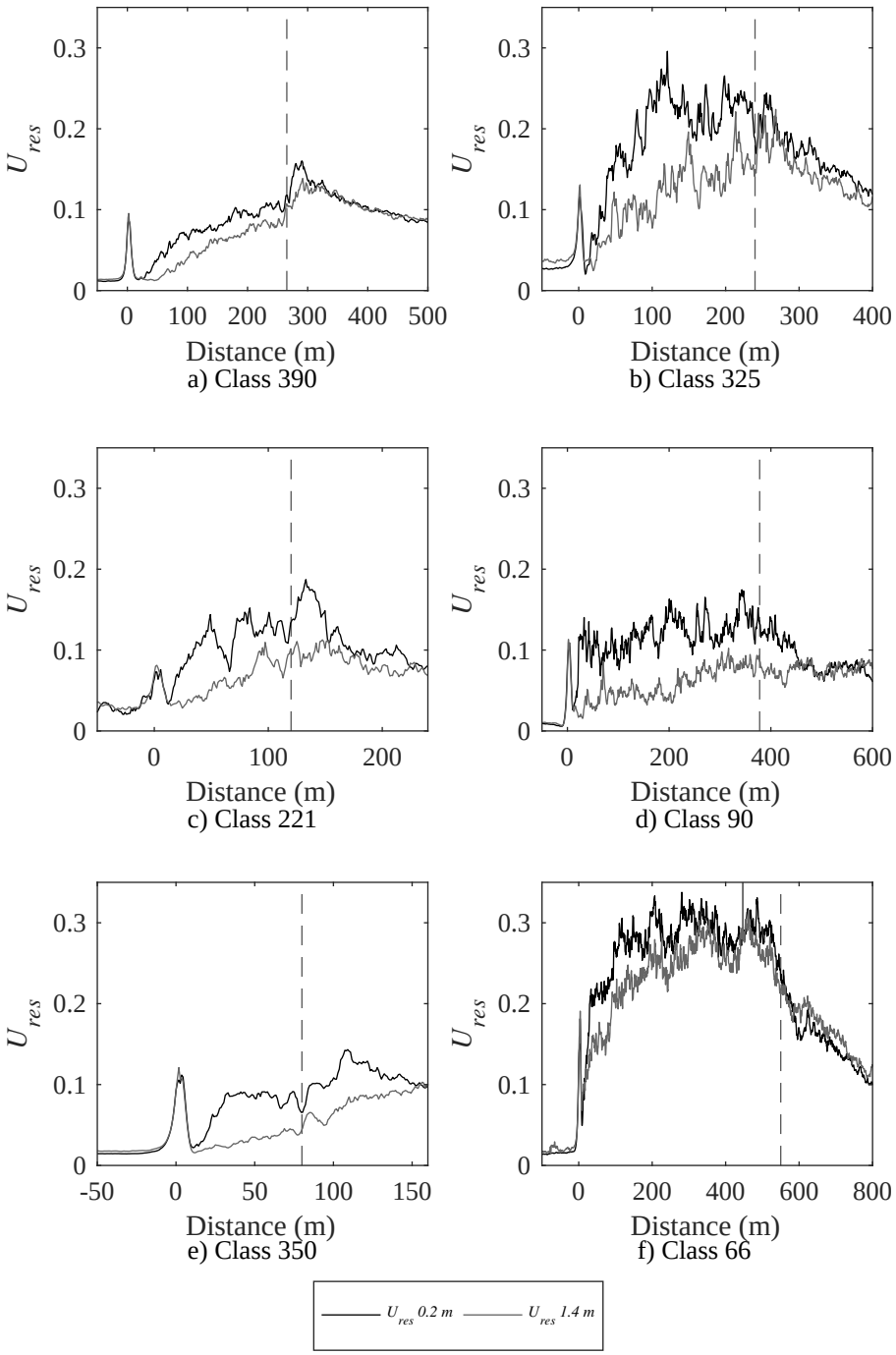

Figure 5: Ensemble U_{res} for all train types analysed. Measurements were made at 0.2 m and 1.4 m above top of rail at a position 3 m from centre of track. The vertical dashed line indicates the train end.

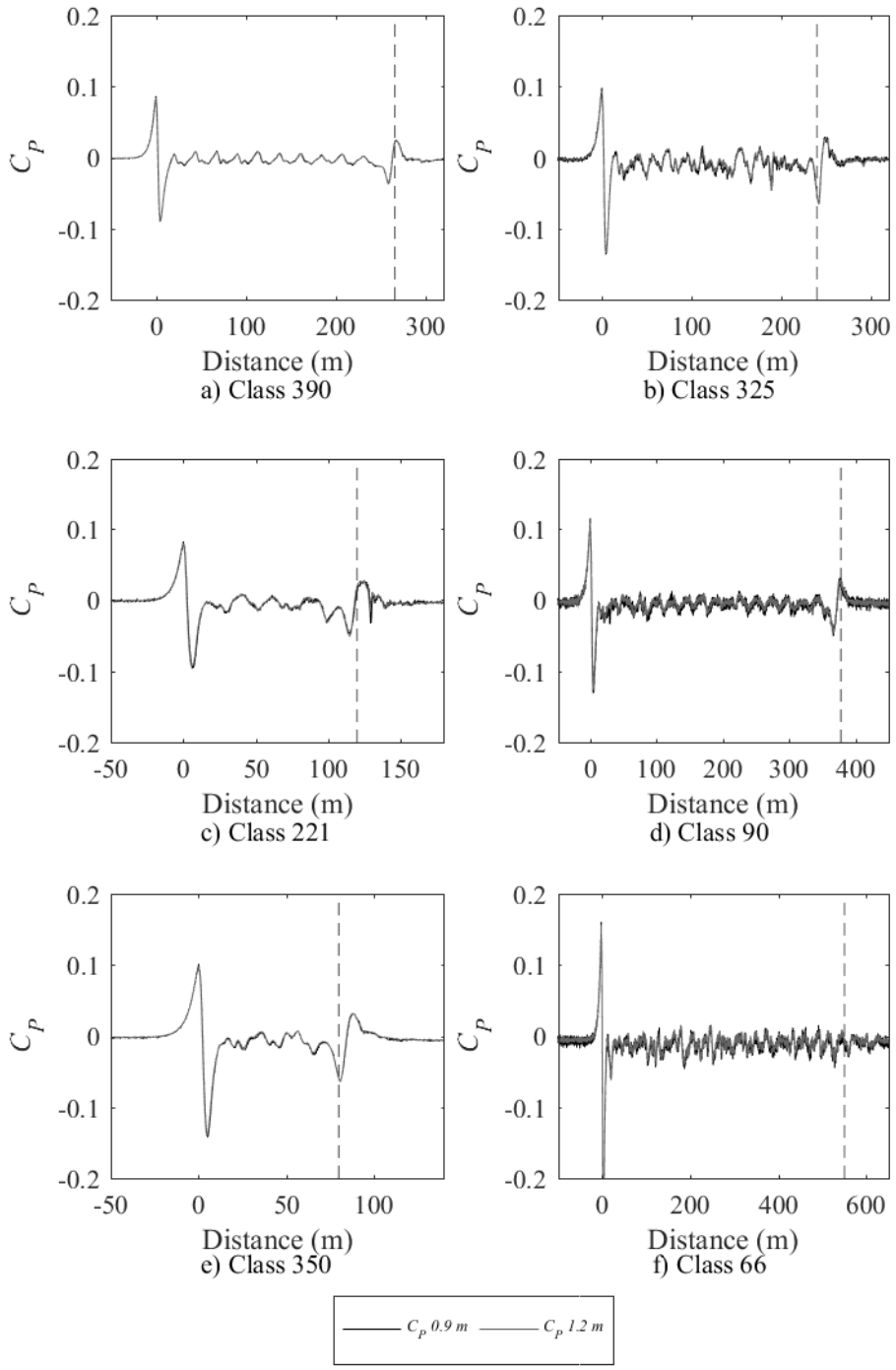

Figure 6: Ensemble C_P for all train types analysed. Measurements were made at 0.9 m and 1.2 m above top of rail at a position 3 m from centre of track. The vertical dashed line indicates the train end.

There are also differences observed between individual types of passenger train and as such it is possible to group these trains into two main types: long distance passenger trains and commuter trains. Commuter trains (Class 350) generally travel short distances, stopping at many stations and with a lower train speed. In many cases this lower speed has led to limited aerodynamic design features for such trains. Long distance passenger trains (Classes 221 and 390) tend to travel over longer distances, making less stops and travel at higher speeds. Such trains are specifically designed for running at higher train speeds and aerodynamic features, such as long nose cones and shielding of undercarriage equipment, have been introduced to increase aerodynamic efficiency, reducing drag and fuel consumption. In terms of aerodynamic development, as observed in figures 5 and 6, the commuter trains tend to have a larger nose peak related to the bluffer nose of the train. Boundary layer development is similar for the 1.4 m measuring position but commuter trains exhibit greater variation. Larger flow magnitudes are recorded initially for the commuter trains at the 0.2 m measuring height; thought to be related to the open bogie and undercarriage region leading to large flow separations and increased turbulence intensities. However, due to much longer train lengths, flow magnitudes recorded at the 0.2 m measuring height continue to increase until the train tail for the long distance passenger train, and as such peak magnitudes towards the rear of the train are larger than those observed for commuter trains. The long nose cone of long distance passenger train has been previously shown to exhibit a large velocity peak at the train tail, created by separation of helical vortex structures which spread into the wake [31, 17]. The relative bluff end of the commuter train does not create such flow features, and as such no large tail peak is observed and the flow just decays into the wake. The general aerodynamic structures and magnitudes presented for the long distance trains agree well with findings in previous studies [5, 25]

Now the general flow development and the differences observed for each train type have been introduced, the finer details of the results are discussed in the following sections.

4.2 TSI analysis

Following on from the general flow development section it is important to conduct a full TSI style analysis of peak velocity magnitudes. The requirement of European homologation has led to the development of the TSI standards, which include a methodology and set of requirements on maximum slipstream velocities in relation to a predetermined limit; aimed at providing standardised regulations to allow interoperability throughout the European rail network. For straight open ballasted track the limit velocity is calculated as [35],

$$u_{2\sigma} = \overline{u_{max}} + 2\sigma \tag{5}$$

where $\overline{u_{max}}$ is the mean dimensional value of all maximum resultant air speed measurements in the x-y plane and σ is the standard deviation. To calculate the TSI limit velocity, firstly for each independent run the resultant velocity of u and v is calculated, then filtered using a 1 second moving average before taking the maximum value of individual runs. These are used to calculate the mean $\overline{u_{max}}$ and standard deviation σ. The documentation states for open track a train running at 160-250 km/h should not cause maximum 1 second moving average velocities exceeding 20.0 m/s at 0.2 m above top of rail and 3.0 m from the centre of the track or 15.5 m/s measured at 1.4 m above top of rail and 3.0 m from the centre of the track [35]. There are additional requirements for trains within the speed range 250-300 km/h such that at 0.2 m above top of rail and 3.0 m from the centre of the track, maximum 1 second moving average velocities should not exceed 22.0 m/s, and

similarly a maximum 1 second moving average velocity 15.5 m/s measured at 1.4 m above top of rail and 3.0 m from the centre of the track [35]. It should be noted that apart from High Speed 1, only the lower limit is applicable on the UK railway network as the maximum train speed is currently 200 km/h and due to low train speeds nominally freight trains are not considered; a point discussed further below.

	Mean value $\overline{u_{max}}$ (m/s)	Standard deviation σ (m/s)	TSI value $u_{2\sigma}$ (m/s)	Dimensionless TSI value $U_{2\sigma}$
Height above TOR (m)	Class 390			
0.2	9.36	1.95	13.26	0.24
1.4	8.23	1.30	10.82	0.19
	Class 221			
0.2	9.30	1.95	13.19	0.24
1.4	7.18	1.18	9.53	0.17
	Class 350			
0.2	6.99	1.53	10.05	0.22
1.4	5.93	1.14	8.12	0.18
	Class 325			
0.2	13.29	1.79	16.86	0.38
1.4	9.30	1.39	12.09	0.27
	Class 90			
0.2	5.55	0.20	5.95	0.18
1.4	3.77	0.59	4.95	0.15
	Class 66			
0.2	13.44	1.10	15.64	0.47
1.4	12.15	1.54	15.22	0.45

Table 4: Results from a TSI analysis for the measuring positions 0.2 m and 1.4 m above TOR at 3 m from COT. The table gives the mean maximum value, the standard deviation and TSI value in both dimensional and non-dimensional form.

The TSI analysis results in table 4 indicate that limit values are not exceeded by any train examined for both measuring heights. As discussed, higher velocity magnitudes are observed at height 0.2 m in comparison to 1.4 m due to exposed bogies and underbody equipment, especially for the commuter and freight trains. Calculated values for standard deviation are similar for all train types, except the Class 90, with smaller values calculated at the 1.4 m measuring height in comparison to 0.2 m, again thought to be related to rough bogie regions. This finding is not true for Classes 66 and 90. Large bluff containers on the Class 66 hauled freight

train lead to large flow separations which may be the reason for higher values measured at 1.4 m, especially given the nature of container loading, and clearly for the Class 90 the small ensemble size has an effect on values calculated; however, the results are presented here for illustrative purposes.

It is striking that some of the highest TSI values are calculated for the freight train even though the train speed is only 60% of the long distance passenger trains, as discussed above. These results are similar to findings in previous studies [5, 7, 30]. As discussed, freight trains are not currently considered as part of the TSI methodology due to the lower train speeds. In the UK however, other controls exist to limit aerodynamic slipstream effects which would be applicable for freight trains. For example RSSB 'RGS RIS-7016-INS: Interface between station platforms, tracks, trains and buffer stops' has methods to control safety between different railway interfaces [2]. At station platforms with passing freight trains actions should be taken to reduce the risks from aerodynamic effects, especially in relation to lightweight objects and vulnerable passengers. In addition, RSSB GI/GN7616 provides a risk assessment methodology to indicate appropriate actions required to mitigate against aerodynamic risks. The results presented here indicate that although the TSI limit values are not broken the largest velocity magnitudes are measured for the Class 66 container freight train. If proposed increases in freight train speeds are implemented then issues could be observed [18], especially in light of recent freight incidents [22, 23].

4.3 Nose shape and length

A breadth of research has shown that the aerodynamic shape and length of a train nose can dramatically alter the pressure wave development as a train enters a tunnel. Indeed, estimates to the magnitude of pressure and velocity peaks have been calculated using 1-dimensional analysis and rely on some sort of shape coefficient

for each train type [36]. A direct comparison of the open air static pressure measured in the nose region for each train type analysed is shown in figure 7. It should be noted that the time scale in this analysis has been normalised with respect to the individual train speed and a nominal length of 4 m to allow ease of comparison between data sets.

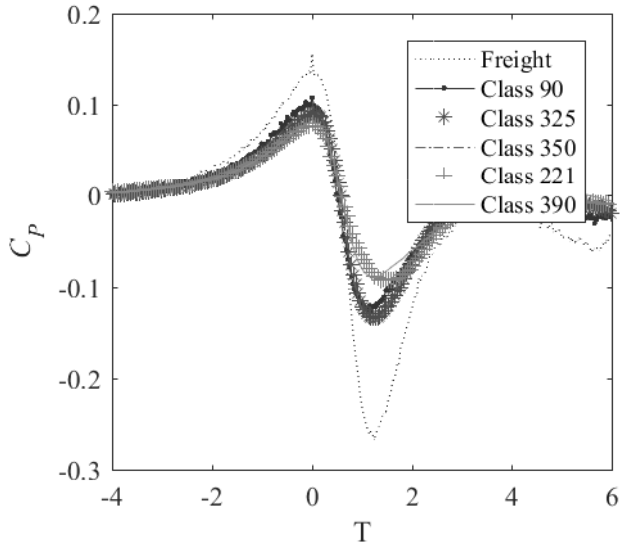

Figure 7: Ensemble C_P traces in the nose region for each train type measured. Measurements were made at 1.2 m above top of rail at a position 3 m from centre of track. The time scale is normalised with respect to the individual train speed and a nominal length scale of 4 m.

Figure 7 indicates that data can be clearly split into the key groups of train type: freight, commuter and long distance passenger. The bluff, sharp edged Class 66 freight locomotive creates the largest peak magnitudes, due to large flow separation from leading edges. The commuter type train has a relatively short train nose ($\sim$1-2 m) but the leading edges are rounded which has the effect of reducing peak magnitudes in comparison to the Class 66 freight locomotive. Although technically a freight train, the Class 325 also follows the trend of the Class 350, as the train design is actually closer to that of a commuter train. The Class 221 and Class

390 passenger trains have the longest train noses with the most aerodynamically designed features. As would be expected the peak magnitudes created by the long distance passenger trains are the lowest of all trains measured. It is interesting to note that peaks magnitudes for both train types are very similar even though the Class 390 train nose is twice as long as the Class 221 nose length, suggesting, at least for open air pressures, that increased nose lengths for aerodynamically designed trains have little effect on pressure development. Although true for the train types considered, this finding is not universal as shown in research by Johnson and Dalley[14], whereby very long train noses were shown to significantly reduce pressure changes.

		0.2 m TOR		1.4 m TOR	
	Nose length (m)	Maximum C_P	Minimum C_P	Maximum C_P	Minimum C_P
Class 390	3.6	0.09	-0.09	0.08	-0.09
Class 221	2.7	0.08	-0.10	0.08	-0.09
Class 350	1.5	0.10	-0.14	0.10	-0.14
Class 325	1.5	0.12	-0.13	0.11	-0.13
Class 90	1.0	0.10	-0.14	0.09	-0.14
Class 66	0.2	0.16	-0.26	0.16	-0.27

Table 6: Maximum and minimum C_P and the assumed train nose length.

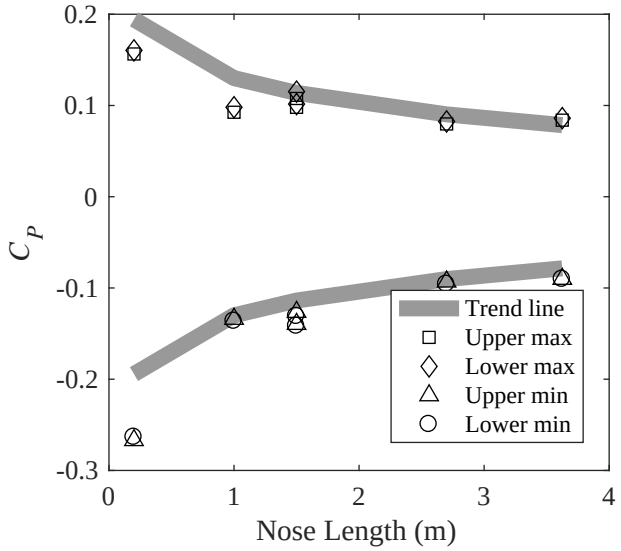

Figure 8: Maximum and minimum C_P magnitudes plotted against nose length.

Plotting the maximum and minimum pressure magnitude, as shown in table 6, against nose length for each train type, shown in figure 8, indicates a clear trend of decreasing peak pressure magnitudes with train nose length. In this instance, the train nose length is defined as the distance from the nose tip at the front of the train to the point at which the main cross-sectional area of the leading vehicle is achieved. There is little difference between the 0.9 m and 1.2 m measuring heights for this lateral position from centre of track, thought to be due to the close positioning of the probes. A full rake of pressure measurement positions, of that outlined in the CEN methodology [9], would provide a much more detailed overview of possible changes in pressure with vehicle height and the effects of vehicle geometry.

Figure 9 shows the ensemble longitudinal and lateral velocities for Classes 66, 350 and 390. The bluff Class 66 nose geometry creates larger peak slipstream magnitudes in comparison to the passenger trains with aerodynamic smoothing features. For each train, in the nose region there is a positive then negative peak in U, characteristic of flow separation leading to a flow reversal in this region. The magnitude of this separation follows the trends laid out previously for the

freight, commuter and long distance passenger trains. This trend is also seen in the lateral velocities V, whereby a peak in velocity in the direction away from the centre of track is observed. Clearly the nose shape and length have a large effect on the aerodynamic flow created in this region, as discussed in previous studies [14, 31, 29]

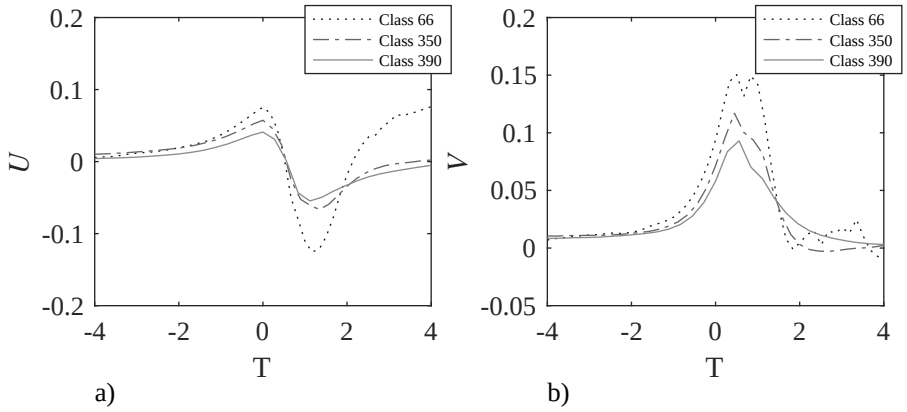

Figure 9: Ensemble U and V traces in the nose region for Classes 66, 350 and 390. Measurements were made at 1.4 m above top of rail at a position 3 m from centre of track. The time scale is normalised with respect to the individual train speed and a nominal length scale of 4 m.

4.4 Effect of train length

It is well known that following the train nose region the aerodynamic flow develops into a thickening boundary layer along the length of the train until the tail region [4]. However, previous studies have not had the opportunity to assess the influence of train length on boundary layer development within specific vehicle classes. Freight trains are nearly always different lengths depending on the number of wagons attached to the lead locomotive(s). There are also a number of passenger trains that vary in length depending on how many carriages are included in the formation, or whether two sets of carriages are joined together. Figures 10 and 11 show comparisons of slipstream velocities and pressure for the same train types but

of different train lengths; it should be noted that the normalised time base in this figure is based on the length of an individual carriage.

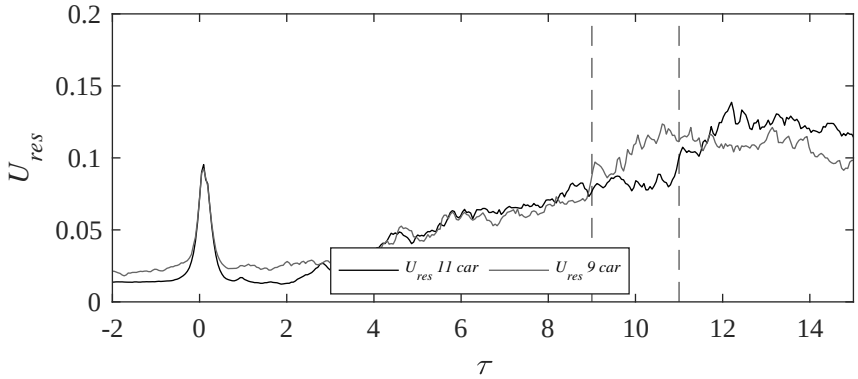

a) Class 390

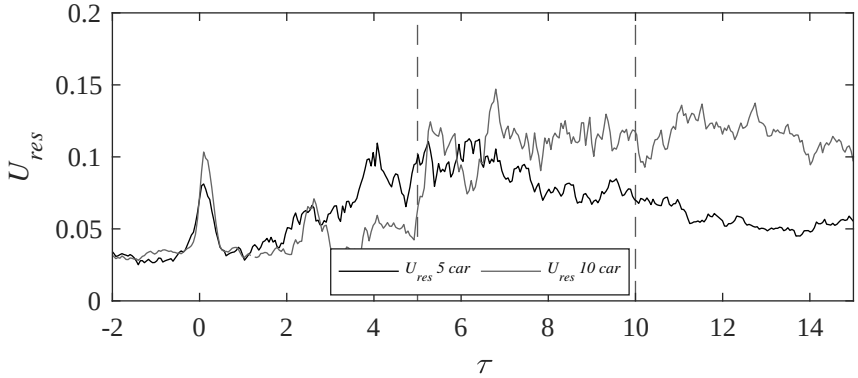

b) Class 221

Figure 10: Ensemble U_{res} for the Class 390 and Class 221 trains of different train lengths. Measurements were made at 1.4 m above top of rail at a position 3 m from centre of track. The vertical dashed line indicates the train end.

Generally for passenger trains the boundary layer growth is seen to increase along the length of the train. The addition of further carriages continues this boundary layer growth, with velocities reaching higher slipstream velocity magnitudes for the longer train. This is particularly important for the Class 390 passenger train where the largest flow peak is observed at the train tail. The tail peak magnitude difference between the 9 and 11 car trains is approximately 10%. Increasing the train length leads to continued boundary layer growth with larger aerodynamic mag-

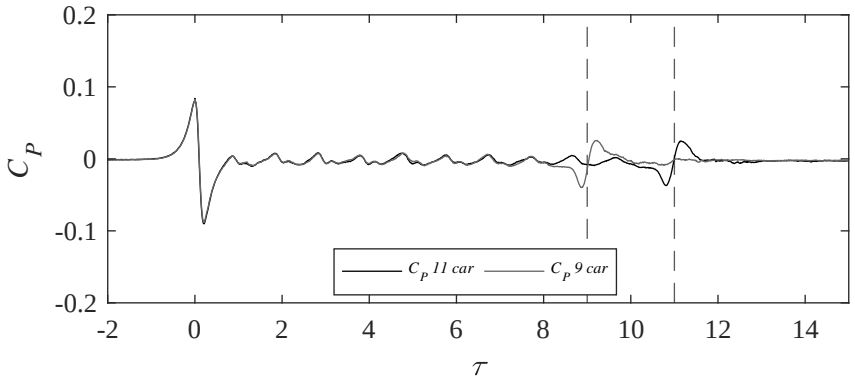

a) Class 390

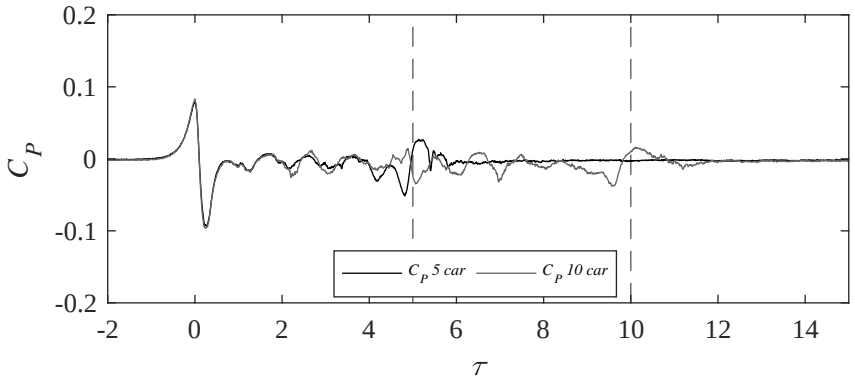

b) Class 221

Figure 11: Ensemble C_P for the Class 390 and Class 221 trains of different train lengths. Measurements were made at 1.2 m above top of rail at a position 3 m from centre of track. The vertical dashed line indicates the train end.

nitudes. This observation is different to findings from previous studies [31, 29], where magnitudes within boundary layer were shown to reach stability punctuated with peaks due to inter-carriage spacing or gaps between containers and inter-wagon spacing on freight trains. Boundary layer growth and near wake flow for trains of different lengths was similar; but interestingly boundary layer growth was seen to stabilise for the longer train closely following the number carriages in the shorter train [31, 29]. It is therefore conceivable that velocity magnitudes within the boundary layer growth will stabilise after a certain length dependent on train type. Theoretically this statement makes sense as the flow entrained in the boundary layer reaches saturation and as such velocities will be limited to a maximum magnitude as the boundary layer growth spreads laterally.

In figure 11, following the nose region there are a series of pressure transients created at the inter-carriage gaps, with a time base related to carriage length. Additional carriages create further transients at inter-carriage gaps, until the train tail where the characteristic change in pressure is of similar magnitude for all train lengths. These additional peaks are important to consider in various aerodynamic load applications, such as trackside structures and people, in relation to fatigue and safety. Indeed, previous studies have observed such effects due to multiple train sets coupled together [11, 25, 28].

The Class 221 passenger train is run as either a set of 5 carriages or two sets of 5 carriages coupled together. The aerodynamically shaped nose of the Class 221 creates a large V-shaped region at the coupling of two 5-carriage sets, which as figure 10 shows clearly affects the aerodynamic flow. The 10 car train has a step slipstream velocity peak coinciding with a characteristic change in pressure at the coupling region. Again, it is important to consider the additional peaks when considering loading applications. These results agree well with work conducted by Guo et al. [11] who concluded that large pressure variations and velocity peaks are

observed in the coupling region between two train sets and that the coupling influences the general flow structure further down the train and into the wake region.

4.5 Correlation of boundary layer gusts

The boundary layer around a train is a highly turbulent flow of many different turbulent scales [4]. Turbulence intensities, calculated from the longitudinal component of slipstream velocity through the ratio of standard deviation with respect to the mean for each train type measured, are shown in figure 12. Results indicate that higher intensities are observed at the lower measuring position in the bogie region due to unshielded bogies. As expected, more aerodynamically designed trains, such as the long distance passenger trains, exhibit lower turbulence intensities due to aerodynamic features associated with carriage design, such as wheel fairings and lower side skirts. The Class 66 freight train exhibits the largest values; however, results are somewhat skewed due to the different container loading configurations and as such results should be treated with a larger degree of uncertainty. Previous studies have shown however that freight trains with standard container loading configurations exhibit high turbulence intensity values due to the sharp edged bluff shape of the locomotive, wagons and containers [29]. It should be noted that the high turbulence intensities measured for the Class 325 are thought to be related to the lower ensemble size in relation to other train types. The Class 325 and 350 underbody equipment placements are relatively similar and as such with a larger ensemble size it would be expected that the turbulence intensity levels for the Class 325 would be similar to the Class 350.

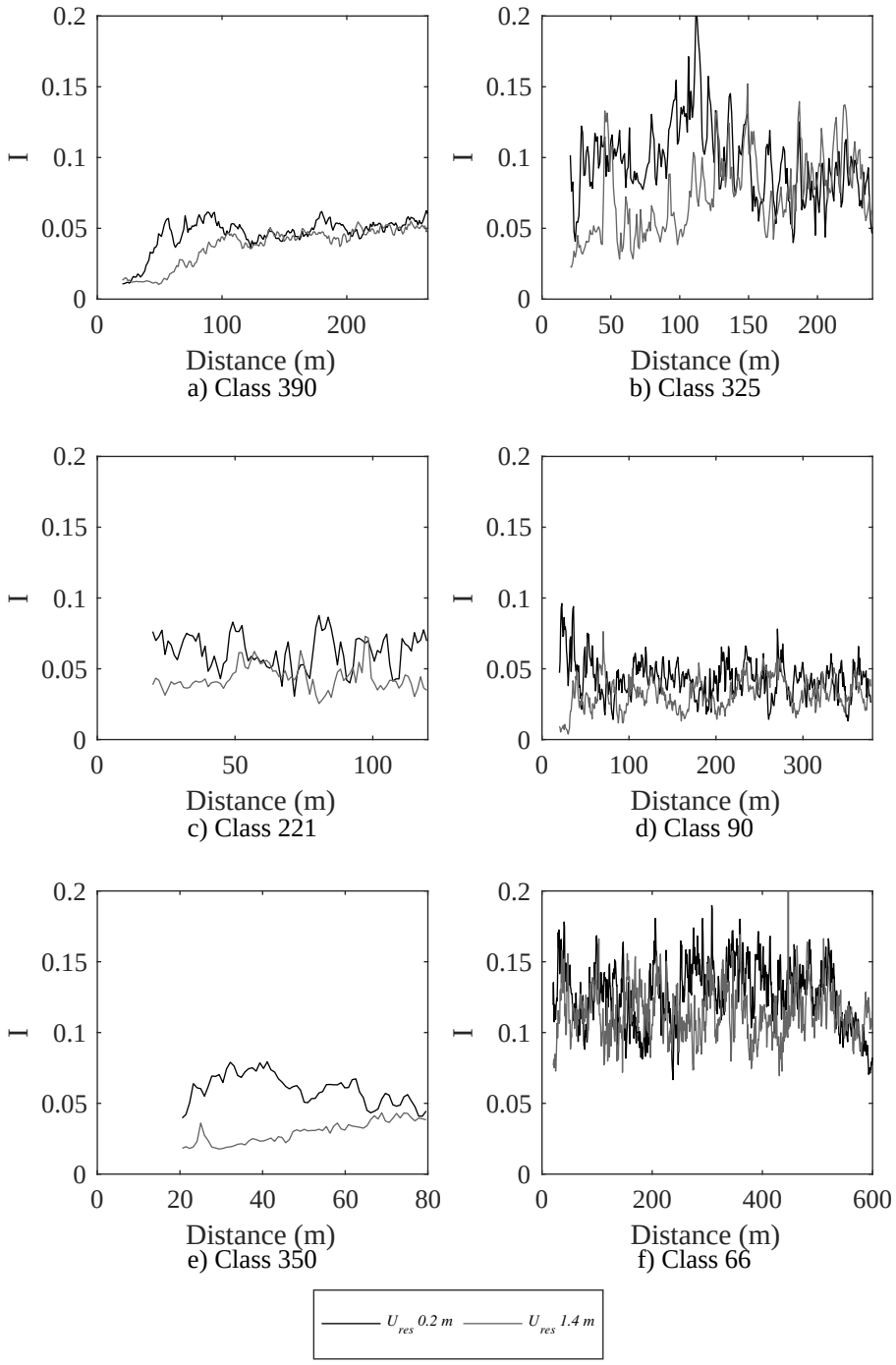

Figure 12: Boundary layer turbulence intensity results for measuring positions 1.4 m and 0.2 m above top of rail and a position 3 m from the centre of track.

Autocorrelation can be used as a measure of dependence of values in a signal

at one time with respect to itself at another time; thus it can be used to detect non-randomness in data. For a time series with constant time step, the lag is number of time steps between the signal and itself in the autocorrelation function. In railway aerodynamics it is usual for the autocorrelation function to be applied to the boundary layer region, usually defined as 20 m from the train nose to the train tail, to calculate the correlation of turbulent fluctuations, providing information about the duration of gusts in this region. It was however found that, for the measuring positions analysed, the boundary layer was still growing along much of the train length and as such the measuring anemometers were becoming more and more submersed in the boundary layer as the train passed. Theoretically this creates an issue for the autocorrelation calculations as the growth implies that the length scale will be potentially changing along the length of the train. This result was more evident for some trains rather than others, namely the long distance passenger trains. The autocorrelation methodology was altered to account for this finding, focusing only on the region were visually the ensemble average slipstream appeared stable for each train type analysed.

Results, shown in figure 13, indicate that much of the energy contained within the boundary layer region is at time scales below 0.5 seconds for all types of train analysed, i.e. high levels of small scale turbulence. Results measured in the bogie region at height 0.2 m fall away more sharply than results from height 1.4 m, indicating higher levels of small scale turbulence related to the aerodynamically unshielded underbody equipment. A Fourier transform was applied to the autocorrelation data which highlighted for the long distance passenger trains peaks in the low frequency range of 2-4 Hz. When this frequency is transformed to a length with respect to train speed, it was found that this length was consistent with that of individual carriage lengths. It is thought that the peaks in the autocorrelation results, shown in figure 13, could be therefore related to slipstream velocity peaks

caused by inter-carriage gaps.

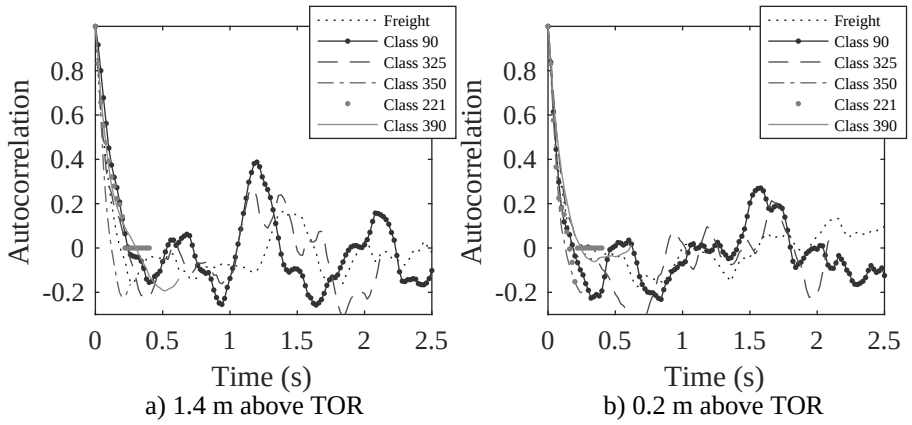

Figure 13: Boundary layer autocorrelation results for measuring positions 1.4 m and 0.2 m above top of rail and a position 3 m from the centre of track.

A useful property of correlograms is that the integral under the curve represents the integral time scale [15]. Discretising the integral, via the trapezium method, under the average autocorrelation from the zero lag to the first zero crossing it is possible to find an estimate of the aerodynamic integral time scale. Multiplying the time scale by train speed gives the integral length scale. Table 8 shows the integral time and length scales for the different trains examined. It is clear that there is some variation between different train types, especially between the passenger and freight trains. In general, for the long distance passenger trains shorter length scales are observed in the bogie region at height 0.2 m, due to the higher levels of small scale turbulence, in relation to the aerodynamically smoothed train side at measuring height 1.4 m. For other train types this distinction between measuring heights is not so clear, possibly due to the lack of aerodynamic smoothing features. Results agree well with previous observations by Sterling et al. [31] who concluded that aerodynamic smoothing features clearly had an effect on the turbulent structures created around the moving train.

Results in table 8 suggest that turbulent length scales are on average within

Train type	Measurement position			
	0.2 m TOR		1.4 m TOR	
	Time scale (s)	Length scale (m)	Time scale (s)	Length scale (m)
Class 390	0.08	4.66	0.09	5.18
Class 221	0.06	3.24	0.09	5.11
Class 350	0.05	2.33	0.05	2.32
Class 325	0.08	3.66	0.08	3.48
Class 90	0.06	2.11	0.11	3.53
Class 66	0.07	2.25	0.07	2.30

Table 8: Autocorrelation integral time and length scales for all train type examined.

the range 3-4 m, similar to the distance between the measuring instrument positions. By applying the method of cross-correlation, to measure the dependence of values in a signal at one time with respect to another signal at another time, it may be possible to pick out whether larger turbulent structures are recorded for multiple measuring positions along the trackside and observe how well correlated these structures are at different times within the boundary layer flow. The results indicated much weaker correlation, as would be expected given the nature of the transient flow. It was however possible to observe a number of key peaks within the individual cross-correlation results, which following a Fourier transform, indicated length scales similar to that of the autocorrletion. Due to this similarity and the lack of additional findings the cross-correlation results are not presented here.

For all trains examined the unshielded bogie region and inter-carriage gap are clearly areas that would lead to large flow separation. The analysed results suggest that increasing velocities in the boundary layer flow at the lower regions examined are primarily driven by flow separation at bogies and inter-carriage gaps and that additional shielding in these regions through aerodynamic fairings would potentially reduce slipstream velocity magnitudes.

5 Conclusions

This paper presents a detailed set of experiments conducted to measure the aerodynamic properties of a cross section of railway vehicles in normal traffic conditions. The large data set has been analysed with respect the variations in vehicle type observed. The results presented offer a number of important findings on railway aerodynamics:

- The variability of freight results was much larger in comparison to the passenger trains examined, caused by the separation of aerodynamic flow structures around the bluff freight train shape, leading to a complex highly turbulent slipstream around the train. Although the train speed is lower for the freight train the magnitude of the flow is larger than observed for the passenger trains.

- It was found that passenger trains could be divided into two main types; long distance passenger trains and commuter trains.

- Commuter trains are generally bluffer in shape and shorter in length. Characteristic flow features include a large nose peak in velocity leading into a typical boundary layer growth to the tail of the train where velocities are seen to decay into the wake. Larger boundary layer velocities were observed at height 0.2 m due to the unshielded bogie region.

- Long distance passenger trains are generally aerodynamically shaped, including underbody shielding, and the longest passenger trains examined. Characteristic flow features include a small nose peak in velocity developing into a typical boundary layer growth. At the tail of the train a large velocity peak is observed due to the separation of helical vortex structures.

- Results from a TSI style analysis were all found to lie below prescribed limit

values; although the freight train results were surprisingly large given the low train speeds in comparison to the long distance passenger trains.

- Peaks in pressure at the train nose can be clearly divided according to train type. The magnitude of flow separation at the train nose was shown to be dependent on train type and nose design.

- The effect of increased train length was shown to increase boundary layer growth and slipstream velocity magnitudes. This was shown to be important for aerodynamically smoothed long distance passenger train as it led to an increased velocity peak at the train tail. Boundary layer stabilisation is not observed as in previous studies.

- Coupling two sets of carriages together creating a large V-shaped region in the centre of the train led to a clear step slipstream velocity peak coinciding with the change in pressure at the coupling region. The coupling influences the general flow structure further down the train and into the wake region.

- Higher turbulence intensities were observed at lower measuring heights due to unshielded bogie regions. Freight trains exhibited the largest turbulence intensities.

- Autocorrelation results indicated the for all train types that much of the energy within the boundary layer region was at time scales below 0.5 seconds, implying high levels of turbulence. Results measured in the bogie region at height 0.2 m fall away more sharply than results from height 1.4 m, indicating higher levels of small scale turbulence related to the aerodynamically unshielded underbody equipment.

- Cross-correlation of results indicated similar results to the autocorrelation time scales for larger scale separation of turbulent structures from bogie and

inter-carriage regions.

Funding

This work was carried out as part of the project 'The measurement of train aerodynamic phenomena in operational conditions' funded by the UK Engineering and Physical Sciences Research Council (Grant EP/I03842X/1).

Acknowledgements

The authors wish to thank Russell Walker from Network Rail and Dr Adam Jackson from the University of Birmingham for their help arranging and conducting the experiment.

References

[1] Real time trains - http://www.realtimetrains.co.uk/.

[2] RSSB RGS RIS-7016-INS: Interface between station platforms, tracks, trains and buffer stops, 2014.

[3] C. J. Baker, S. J. Dalley, T Johnson, A Quinn, and N. G. Wright. The slipstream and wake of a high-speed train. *Proceedings of the Institution of Mechanical Engineers, Part F: Journal of Rail and Rapid Transit*, 215(2):83–99, 2001.

[4] Chris Baker. The flow around high speed trains. *Journal of Wind Engineering and Industrial Aerodynamics*, 98(6-7):277 – 298, 2010. 6th International Colloquium on Bluff Body Aerodynamics and Applications.

[5] Chris J Baker, Andrew Quinn, Mikael Sima, Lars Hoefener, and Ricardo Licciardello. Full-scale measurement and analysis of train slipstreams and wakes. part 1: Ensemble averages. *Proceedings of the Institution of Mechanical Engineers, Part F: Journal of Rail and Rapid Transit*, 228(5):451–467, 2014.

[6] J.R. Bell, D. Burton, M. Thompson, A. Herbst, and J. Sheridan. Wind tunnel analysis of the slipstream and wake of a high-speed train. *Journal of Wind Engineering and Industrial Aerodynamics*, 134:122 – 138, 2014.

[7] J.R. Bell, D. Burton, M.C. Thompson, A.H. Herbst, and J. Sheridan. Moving model analysis of the slipstream and wake of a high-speed train. *Journal of Wind Engineering and Industrial Aerodynamics*, 136:127 – 137, 2015.

[8] CEN European Standard. EN 14067-6 Railway applications - Aerodynamics Part 6: Requirements and test procedures for cross wind assessment. Technical report, CEN, 2010.

[9] CEN European Standard. EN 14067-4 Railway applications - Aerodynamics Part 4: Requirements and test procedures for aerodynamics on open track. Technical report, CEN, 2013.

[10] P. Deeg, M. Jönsson, H.J. Kaltenbach, M. Schober, and M. Weise. Cross-comparison of measurement techniques for the determination of train induced aerodynamic loads on the track bed. In *Proceedings of the BBAA VI, Milano, Italy*, 2008.

[11] Zi-Jian Guo, Tang-Hong Liu, Zheng-Wei Chen, Tai-Zhong Xie, and Zhen-Hua Jiang. Comparative numerical analysis of the slipstream caused by single and double unit trains. *Journal of Wind Engineering and Industrial Aerodynamics*, 172:395 – 408, 2018.

[12] Hassan Hemida, Chris Baker, and Guangjun Gao. The calculation of train slipstreams using large-eddy simulation. *Proceedings of the Institution of Mechanical Engineers, Part F: Journal of Rail and Rapid Transit*, 228(1):25–36, 2014.

[13] Hassan Hemida and Siniša Krajnović. Les study of the influence of the nose shape and yaw angles on flow structures around trains. *Journal of Wind Engineering and Industrial Aerodynamics*, 98(1):34 – 46, 2010.

[14] T. Johnson and S. Dalley. 1/25 scale moving model tests for the transaero project. In Burkhard Schulte-Werning, Rémi Grégoire, Antonio Malfatti, and Gerd Matschke, editors, *TRANSAERO — A European Initiative on Transient Aerodynamics for Railway System Optimisation*, pages 123–135, Berlin, Heidelberg, 2002. Springer Berlin Heidelberg.

[15] P. K. Kundu and I. M. Cohen. *Fluid Mechanics*. Academic Press, San Diego, CA, 2010.

[16] P Moran and R P Hoxey. A probe for sensing static pressure in two-dimensional flow. *Journal of Physics E: Scientific Instruments*, 12(8):752, 1979.

[17] T.W. Muld. Analysis of Flow Structures in Wake Flows for Train Aerodynamics. Technical report, Royal Institute of Technology, Department of Mechanics, SE-100 44 Stockholm, Sweden, 2010.

[18] Network Rail. Freight network study, https://www.networkrail.co.uk/wp-content/.../freight-network-study-april-2017.pdf, 2017.

[19] Jan Östh and Siniša Krajnović. A study of the aerodynamics of a generic container freight wagon using large-eddy simulation. *Journal of Fluids and Structures*, 2013.

[20] C Pope. Safety of slipstreams effects produced by trains. *A report prepared by Mott Macdonald, Ltd., for RSSB*, 2006.

[21] A. D. Quinn, M. Hayward, C. J. Baker, F. Schmid, J. A. Priest, and W. Powrie. A full-scale experimental and modelling study of ballast flight under high-

speed trains. *Proceedings of the Institution of Mechanical Engineers, Part F: Journal of Rail and Rapid Transit*, 224(2):61–74, 2010.

[22] Rail Accident Investigation Branch. Report 01/2017: Wheelchair contacting a train at twyford station, https://www.gov.uk/government/news/report-012017-wheelchair-contacting-a-train-at-twyford-station. Technical report, Rail Accident Investigation Branch, 2017.

[23] Railway Safety and Standards Board. Parents alerted to pushchair risk on platforms, https://www.rssb.co.uk/news/pages/parents-alerted-to-pushchair-risk-on-platforms.aspx, 2017.

[24] P.R. Rigby. Slipstream effects of aerodynamically rough trains (tm-aero-60). Technical report, British Rail Research, 1982.

[25] D. Rocchi, G. Tomasini, P. Schito, and C. Somaschini. Wind effects induced by high speed train pass-by in open air. *Journal of Wind Engineering and Industrial Aerodynamics*, 173:279 – 288, 2018.

[26] B. Schulte-Werning, G. Matschke, R. Gregoire, and T. Johnson. RAPIDE: A project of joint aerodynamics research of the European high-speed rail operators. In *World Congress on Railway Research*, pages 19–23, 1999.

[27] D. Soper, C. Baker, A. Jackson, D.R. Milne, L. Le Pen, G. Watson, and W. Powrie. Full scale measurements of train underbody flows and track forces. *Journal of Wind Engineering and Industrial Aerodynamics*, 169:251 – 264, 2017.

[28] D. Soper, S. Gillmeier, C. Baker, T. Morgan, and L. Vojnovic. Aerodynamic forces on railway acoustic barriers. *Journal of Rail and Rapid Transit*, 2018.

[29] David Soper, Chris Baker, and Mark Sterling. Experimental investigation of the slipstream development around a container freight train using a moving

model facility. *Journal of Wind Engineering and Industrial Aerodynamics*, 135:105 – 117, 2014.

[30] David Soper, Martin Gallagher, Chris Baker, and Andrew Quinn. A model-scale study to assess the influence of ground geometries on aerodynamic flow development around a train. *Proceedings of the Institution of Mechanical Engineers, Part F: Journal of Rail and Rapid Transit*, 2016.

[31] M Sterling, C J Baker, S C Jordan, and T Johnson. A study of the slipstreams of high-speed passenger trains and freight trains. *Proceedings of the Institution of Mechanical Engineers, Part F: Journal of Rail and Rapid Transit*, 222(2):177–193, 2008.

[32] J. Temple and S. Dalley. RAPIDE Project; Analysis of the slipstream data. AEA Technology Rail AEATR-T&S-2001-197. Technical report, AEA Technology Rail, 2001.

[33] J Temple and T Johnson. Review of slipstream effects on platforms. *Rail Safety and Standards Board*, (1), 2003.

[34] J. Temple and T. Johnson. Effective management of risk from slipstream effects at trackside and on platforms. Technical report, A report produced for Rail Safety and Standards Board, August 2008.

[35] TSI. COMMISSION REGULATION (EU) No 1302/2014 concerning a technical specification for interoperability relating to the rolling stock - locomotives and passenger rolling stock subsystem of the rail system in the European Union. Technical report, Official Journal of the European Union, 2014.

[36] AE Vardy, R Sturt, CJ Baker, and D Soper. The behaviour of long entrance hoods for high speed rail tunnels. In *ISAVFT-2015. 16th International Sym-*

posium on Aerodynamics, Ventilation & Fire in Tunnels, Seattle, USA, pages 449–466. BHR Group, Cranfield, UK, 15-17 September 2015.

[37] MARCO Weise, A Orellano, and M Schober. Slipstream velocities induced by trains. *WSEAS Transactions on Fluid Mechanics*, 1(6):759, 2006.